Since January 2020 Elsevier has created a COVID-19 resource centre with free information in English and Mandarin on the novel coronavirus COVID-19. The COVID-19 resource centre is hosted on Elsevier Connect, the company's public news and information website.

Biosensors and Bioelectronics 192 (2021) 113499

Contents lists available at ScienceDirect

Biosensors and Bioelectronics

journal homepage: www.elsevier.com/locate/bios

Bioaerosol monitoring by integrating DC impedance microfluidic cytometer with wet-cyclone air sampler

Chang Heon Lee [a,1], Hyunho Seok [b,1], Woohyuk Jang [a,1], Ji Tae Kim [a], Geunsang Park [c], Hyeong-U Kim [d], Jihun Rho [a], Taesung Kim [b,c,**], Taek Dong Chung [a,*]

[a] Department of Chemistry, Seoul National University, Seoul, 08826, Republic of Korea
[b] SKKU Advanced Institute of Nanotechnology (SAINT), Sungkyunkwan University, Suwon, 16419, Republic of Korea
[c] School of Mechanical Engineering, Sungkyunkwan University, Suwon, 16419, Republic of Korea
[d] Plasma Engineering Laboratory, Korea Institute of Machinery and Materials, Daejeon, 32103, Republic of Korea

ARTICLE INFO

Keywords:
Bioaerosol
Wet-cyclone
Bacteria
Microfluidic chip
Cytometry
DC impedance analysis

ABSTRACT

The recent outbreak of COVID-19 has highlighted the seriousness of airborne diseases and the need for a proper pathogen detection system. Compared to the ample amount of research on biological detection, work on integrated devices for air monitoring is rare. In this work, we integrated a wet-cyclone air sampler and a DC impedance microfluidic cytometer to build a cyclone-cytometer integrated air monitor (CCAM). The wet-cyclone air sampler sucks the air and concentrates the bioaerosols into 10 mL of aqueous solvent. After 5 min of air sampling, the bioaerosol-containing solution was conveyed to the microfluidic cytometer for detection. The device was tested with aerosolized microbeads, dust, and *Escherichia coli* (*E. coli*). CCAM is shown to differentiate particles from 0.96 to 2.95 μm with high accuracy. The wet cyclone air-sampler showed a 28.04% sampling efficiency, and the DC impedance cytometer showed 87.68% detection efficiency, giving a total of 24.59% overall CCAM efficiency. After validation of the device performance, CCAM was used to detect bacterial aerosols and their viability without any separate pretreatment step. Differentiation of dust, live *E. coli*, and dead *E. coli* was successfully performed by the addition of BacLight bacterial viability reagent in the sampling solvent. The usage could be further extended to detection of specific species with proper antibody fluorescent label. A promising strategy for aerosol detection is proposed through the constructive integration of a DC impedance microfluidic cytometer and a wet-cyclone air sampler.

1. Introduction

The recent COVID-19 pandemic has struck globally and the world is still recovering from its impact. Pandemic has harassed mankind since the advent of civilization. Millions of people die at every incidence of pandemic and billions of dollars are spent on response and research. Finding a cure for a pandemic not only incurs massive costs but also requires years of research and clinical trials. Until a cure is found, minimizing the spread of pathogens with biosurveillance is the best approach against pandemics. Biosurveillance refers to the systematic monitoring of all data related to biological threats. This includes continually sampling air or environmental sources and testing them for biological agents (Kman and Bachmann, 2012; Minogue et al., 2019). The early detection of pathogens in air samples could be used to quarantine people or places to prevent further spread of the diseases. Therefore, an effective detection method for bioaerosols, through which most airborne infections occur, is required (Kalogerakis et al., 2005; Nazaroff, 2016). Despite the ample amount of research on air sampling and biological detection methods, only a few have tried to integrate the methods to create bioaerosol detection platforms. Bioaerosol detection has not been standardized or established let alone applicable in the field (Caruana, 2011; Huffman et al., 2020).

Bioaerosols are airborne collections of biological materials. They are first collected with an air sampler in a liquid state, and the collected liquid sample is then analyzed by microscopy, culture techniques, polymerase chain reaction (PCR), or enzyme-linked immunosorbent assays

* Corresponding author.
** Corresponding author.
E-mail addresses: tkim@skku.edu (T. Kim), tdchung@snu.ac.kr (T.D. Chung).
[1] Authors contributed equally to this work.

https://doi.org/10.1016/j.bios.2021.113499
Received 24 March 2021; Received in revised form 27 June 2021; Accepted 8 July 2021
Available online 13 July 2021

(ELISA) (Huffman et al., 2020; Xu et al., 2011). However, these methods either require trained operators or take a prolonged period to obtain results, which makes it unsuitable for real-time monitoring (Choi et al., 2014; Ghosh et al., 2015). For example, PCR, which is the basis for patient diagnosis of COVID-19, requires skilled personnel to work for hours to days to obtain the result (Morales-Narváez and Dincer, 2020). Complex experimental procedures also make it difficult to integrate these methods with air samplers. Fluorescence-activated cell sorting (FACS) is another widely used method for counting and detecting microorganisms (Chen and Li, 2005; Lange et al., 1997; Prigione et al., 2004). FACS is intrinsically adequate for real-time detection because it does not require an incubation period and retains sensitivity due to its particle-by-particle analysis principle. However, the high cost and bulkiness of the FACS device is problematic for its use as a bio-surveillance method (Joo et al., 2010). A breakthrough is being made with the introduction of microfluidics-based devices that are small, inexpensive, and easy to integrate with other operational components such as valves, pumps, mixers, and detectors (Ateya et al., 2008; Kim et al., 2009; McClain et al., 2001; Shrirao et al., 2018; Whitesides, 2006). Real-time bioaerosol detection was demonstrated through a micro-optofluidic platform, which was essentially a miniaturization of FACS device (Choi et al., 2015).

This platform can be further improved by incorporating a DC impedance unit for particle sizing. Although an optical scatter signal is frequently used for particle sizing, its correlation with particle size is intrinsically non-monotonic (Liu and Daum, 2000; Stier and Quinten, 1998). This makes it necessary to perform calibration using standard particles, which is still not accurate because of the differences in refractive indices of standard particles and target particles (Rosenberg et al., 2012). However, the peak magnitude of DC impedance is proportional to the volume of particles regardless of refractive indices (Hurley, 1970; Qin et al., 2011). The DC impedance detection unit offers more reliable particle size information than the optical scattering unit (Miller and Limes, 1988). It is also much smaller, cheaper, and requires a less complicated setup. The DC impedance detection unit has been successfully introduced for measuring particle size but has never targeted airborne particles as of yet (Choi et al., 2013; Chun et al., 2005; Fu et al., 2017; Guo et al., 2015a; Kim et al., 2009; Ren et al., 2016; Shrirao et al., 2018).

In this work, we integrated the wet-cyclone air sampler and DC impedance microfluidic cytometer to develop an integrated system for detecting airborne bacteria without any pretreatment step. The cyclone air sampler is frequently used for its high collection efficiency, high flow rate, portability, and compatibility with quantification methods (Kim et al., 2018; Sung et al., 2017). A commercial wet cyclone (Coriolis μ) and DC impedance microfluidic cytometer are combined to construct an easy, simple, and accurate detection platform for bioaerosol detection. The collection efficiency and size measuring capability of the integrated device is verified. Then, we show that the proposed system can detect and differentiate mineral dust, live *Escherichia coli* (*E. coli*), and dead *E. coli* without any separate pretreatment step.

2. Material and methods

2.1. Bioaerosol generation and chambers

E. coli BL21 was grown on a lysogeny broth (LB) (carbenicillin) plate for 14 h. A single colony was picked and incubated in 100 mL of LB (carbenicillin) medium at 37 °C and 250 rpm until the optical density at 600 nm reached 0.6, as detected with a UV/Vis spectrophotometer (Biodrop DUO; U.K.). The resulting solution was redistributed into 50 mL centrifuge tubes and centrifuged at 10,000 rpm for 10 min at 4 °C. The supernatant was removed, and the residue was then resuspended in 40 mL of Dulbecco's phosphate-buffered saline (DPBS; Welgene, Korea) and incubated at 25 °C for 1 h. The incubated sample was centrifuged at 10,000 rpm for 10 min at 4 °C. The supernatant was removed, and the resulting pellet was resuspended in 20 mL of DPBS.

The generation and sampling of bioaerosol were carried out in an air chamber with a volume of 125 L ($0.5 \times 0.5 \times 0.5$ m^3) as shown in Fig. 1. To prevent outward spreading during the experiments, a high-efficiency particulate air (HEPA) filter was constructed beside the wall of the air chamber. The 2.07 μm bead suspension (Bangs laboratory, 20 mL, 5×10^7 particles mL^{-1}) or bacterial suspension (20 mL, 10^7 cells mL^{-1}) was aerosolized using a 6-jet collision nebulizer (BGI, USA). Aerosolization was performed using a 4 L min^{-1} flow of filtered air, which was controlled using a mass flow controller (VICD220; MFC Korea, Korea). The aerosolization time was adjusted by considering the required concentration of aerosol particles. The generated aerosol was dried by a diffusion dryer. Inside the chamber, air fans were used for homogeneity. The air inside the chamber was maintained at 25 °C and a relative humidity of 50% using a thermo-hygrostat.

2.2. Airborne bacteria collection and detection setup

The system was built by combining a wet cyclone sampler for bioaerosol collection and a microfluidic cytometer for bacterial detection. The wet cyclone aerosol sampler (Coriolis μ; Bertin Technologies, France) was connected to an air chamber, as shown in Fig. 1. The cone of the sampler was filled with 10 mL of DPBS. The sampling time for all experiments was 5 min at an airflow rate of 300 L min^{-1}. The cone was cleaned with 70% aqueous ethanol after each sampling. The collected solution in the air sampler was transferred to a syringe pump for detection. The solution in the syringe pump (Cadent 3; IMI Norgren, Germany) was transferred to a microfluidic cytometer and measured using a microfluidic cytometry system.

An aerosol spectrometer (Model 1.109; Grimm, USA) was used along with the cyclone sampler to measure the concentration of particles in the relevant size range of 0.265–34.0 μm. The aerosol chamber was wiped with ethanol and flushed with filtered air for 10 min (4 L min^{-1}) to remove aerosols from previous experiments.

2.3. Sample preparation

Fluorescent microbeads (Bangs Laboratory) were used to evaluate the performance of the system. The average diameters of the microbeads were 0.96, 2.07, and 2.95 μm, comparable to that of *E. coli*. The microbeads were diluted with DPBS before use.

2.4. Fabrication of microfluidic cytometer

The fabrication process of the microfluidic cytometer was similar to the photolithographic techniques in our previous reports (Choi et al, 2013, 2014). In brief, glass slides (Marienfeld Laboratory Glassware) were cleaned in piranha solution (H_2SO_4:H_2O_2 = 3:1) for 30 min, then rinsed with deionized (DI) water, acetone (CMOS grade, J. T. Baker), and methanol (CMOS grade, J. T. Baker) three times. Cleaned glass slides were spin-coated with hexamethyldisilazane (HMDS; Merck, Kenilworth, NJ, USA) at 6000 rpm for 30 s. The HMDS-coated slides were placed on a hot plate at 110 °C for 1.5 min and subsequently cooled at room temperature for 1 min. Subsequently, a photoresist (PR) AZ9260 (Merck, Kenilworth, NJ, USA) was spin-coated onto the surface of the glass slide using a spin coater at 6000 rpm for 30 s. The PR-coated slides were placed on a hot plate at 110 °C for 1.5 min and cooled at room temperature for 15 min. The slides were aligned under a film photomask and exposed to UV light (365 nm, 18 mJ cm^{-2}) for 25 s with a UV aligner (Midas System Co., Ltd., Korea). The UV-exposed slides were immersed in an AZ400K developer (Merck, Kenilworth, NJ, USA) to develop UV-exposed PR. The glass slides were washed with DI water and dried in clean air. Next, the slides were hard-baked at 150 °C for 15 min. After cooling to room temperature, the slides were etched for 7 min using a 6:1 buffered oxide etch (BOE) solution (J. T. Baker) and cleaned with DI water using an ultrasonic cleaner (351OE-DTH, Branson) for 15 min to

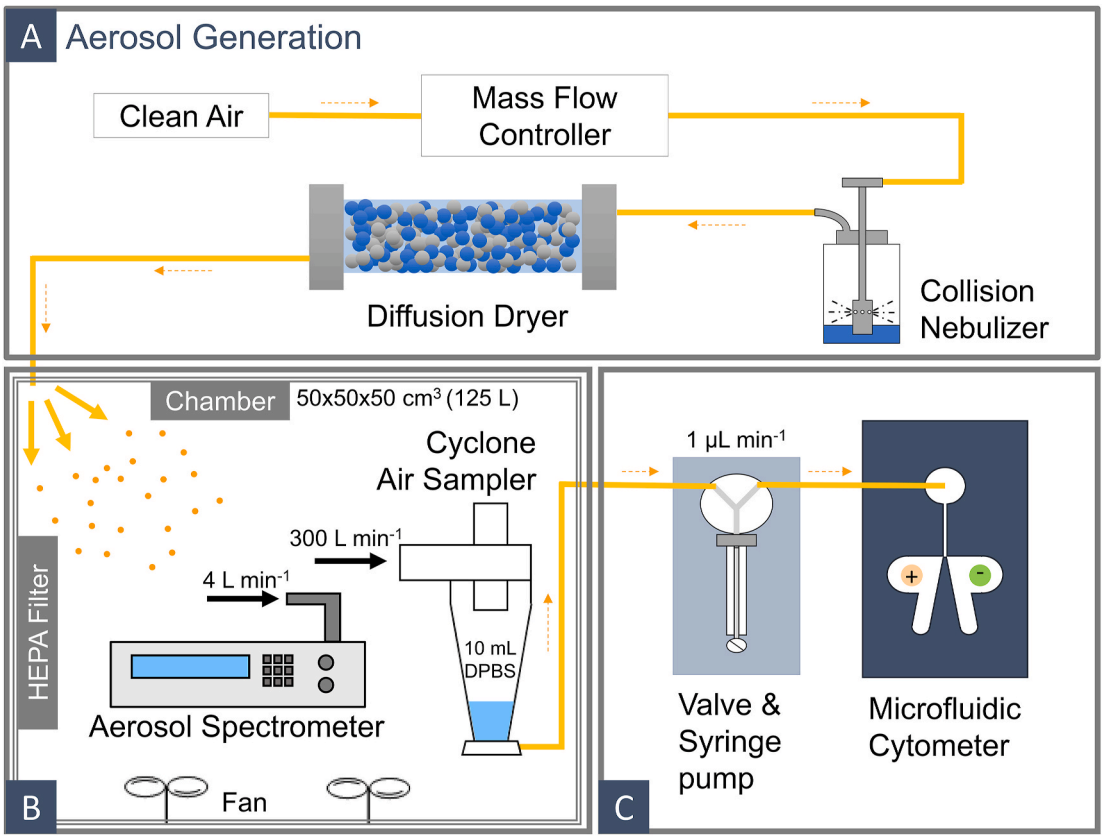

Fig. 1. Bioaerosol collection and detection set-up.

remove impurities from the channel. The patterned slides were drilled to create inlet and outlet holes using a 1 mm drill bit, followed by thermal bonding to the patterned glass in a furnace. The microfluidic channel was cleaned and filled with 0.1 M KCl.

2.5. Microfluidic cytometry

An external custom-made circuit generated a 0.8 V DC bias applied between two Ag/AgCl electrodes and detected the impedance change between the microfluidic channels. The DC impedance-analyzing circuit removed the DC component, and the operational amplifier components in the circuit amplified the impedance signal. For the simultaneous measurement of fluorescence and DC impedance, blue light was focused on the detection region using an objective lens (40×, Nikon). The fluorescence signal was optically filtered using 530/43 band-pass filters and detected using photomultiplier tube (PMT; Hamamatsu, Japan). The impedance and fluorescence signals were transmitted through a data acquisition card (USB-X-6356, National Instruments) with 30 kHz sampling rates. The signals of the particles were saved and matched using a self-programmed LabVIEW (LabVIEW, 2015; National Instrument) program. The particles were infused into a microfluidic cytometer using a syringe pump (Cadent 3; IMI Norgren, Germany) at a flow rate of 1 μL min^{-1}. The syringe pump and microfluidic cytometer were connected by 100 μm diameter glass capillary tubing with Nano Port Assemblies (IDEX, USA).

3. Results and discussion

3.1. Bioaerosol sampling operation

The simulation of the air sampler at different flow rates is shown in Fig. S1. A flow rate of 300 L min^{-1} resulted in a cut-off diameter of 0.3 μm, which is small enough to capture particles covering most of the range of bacteria (Levin and Angert, 2015). Accordingly, the wet cyclone air sampler was operated at a flow rate of 300 L min^{-1} in all subsequent experiments.

The concentration of particles in the range of 1–3 μm inside the air chamber was measured using an aerosol spectrometer, as shown in Fig. 2. The aerosolization period is colored in yellow and the air sampling period is colored in orange. Particles were observed for 15 min, and for the first 10 min, different solutions were aerosolized. When DI water was aerosolized, there was no change in the concentration of 1–3 μm particles for the entire 10 min, as shown in Fig. 2(a). Fig. 2(b) shows 2.07 μm beads in DI water aerosolized for 10 min. A noticeable increase in the particle count indicates that the 2.07 μm beads are aerosolized as expected. Fig. 2(c) shows the case of 2.07 μm beads aerosolized for 10 min and subsequently air-sampled for 5 min. The graph shows that the beads were effectively eliminated from the air. A similar approach was adopted for *E. coli*, but the spectrometer signal from DPBS was so high that the signal from *E. coli* was undistinguishable from the DPBS signal, as shown in Fig. 2(d).

3.2. Operation principle of DC impedance-based cytometer

A two-channel microfluidic cytometer was designed and fabricated to detect bioaerosols collected from an air sampler, as shown in Fig. 3. The cytometer was based on our previous design and was improved to serve our purpose (Choi et al., 2014; Joo et al., 2010). A syringe pump drives the sample solution from the wet cyclone air sampler into the microfluidic cytometer. The sample solution injected through the inlet reservoir passed through a split channel where impedance and fluorescence sensing were performed. Each microfluidic sensing channel was 30 μm in length and 10 μm in width and depth. At the end of each channel, the Ag/AgCl electrode was located for ionic current measurement, as shown in Fig. 3(b). A constant DC voltage of 0.8 V was applied between the two Ag/AgCl electrodes, and the chloride ion flow

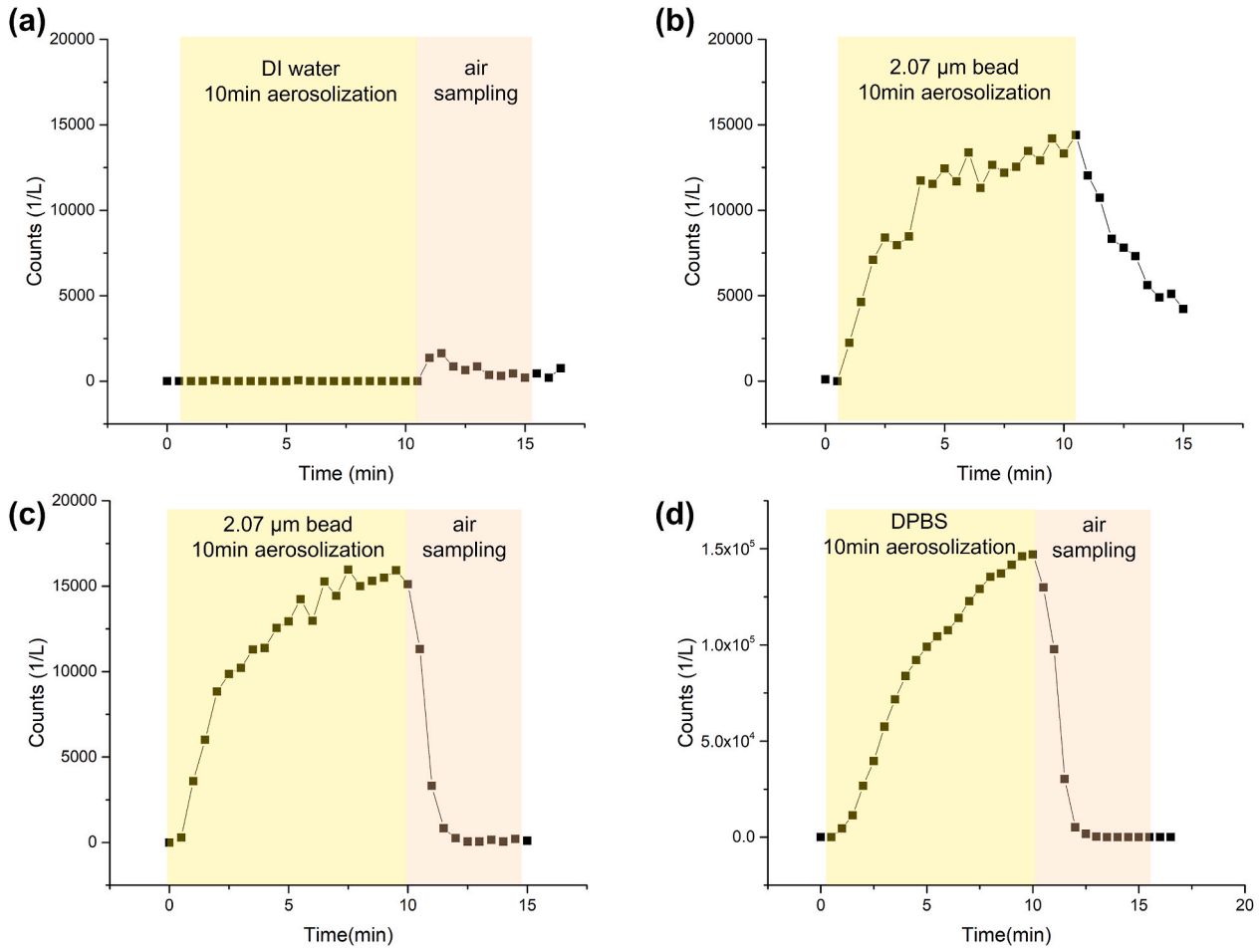

Fig. 2. Spectrometer measurements of different samples in a chamber during aerosolization and air sampling plotted against time with aerosolization period (yellow region) and air sampling period (orange region). (a) Aerosolization of D.I. water for 10 min and subsequent air sampling for 5 min. (b) Aerosolization of 5×10^7 mL^{-1} 2.07 μm bead in DI water for 10 min without air sampling. (c) Aerosolization of 5×10^7 mL^{-1} 2.07 μm bead in DI water for 10 min and subsequent air sampling for 5 min. (d) Aerosolization of DPBS for 10 min and subsequent air sampling for 5 min. (For interpretation of the references to color in this figure legend, the reader is referred to the Web version of this article.)

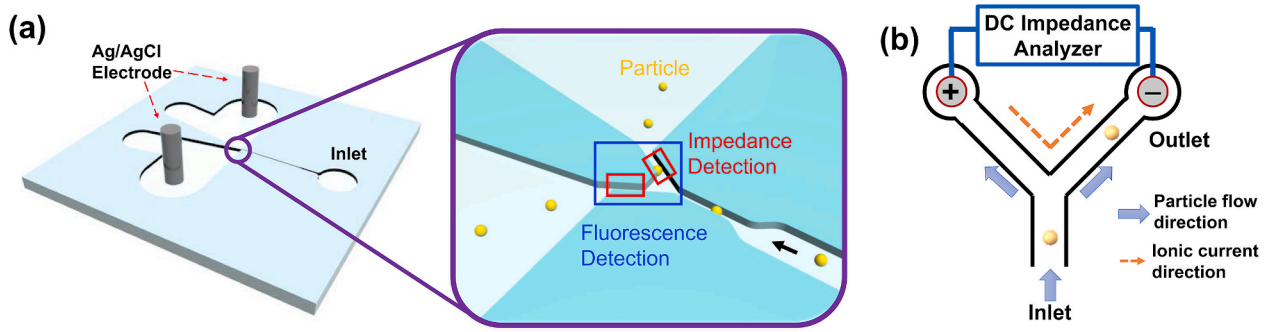

Fig. 3. (a) Two-channel microfluidic cytometer and magnified part of the microfluidic sensing channel. The impedance measurement region (red rectangles) and the fluorescent measurement region (blue rectangle) enables the simultaneous detection of DC impedance and fluorescence. (b) Simplified diagram of microfluidic cytometer expressing the origin of current signal. (For interpretation of the references to color in this figure legend, the reader is referred to the Web version of this article.)

produced an ionic current. As particles pass through the sensing region, they block the narrow channel interfering with chloride flow, resulting in a decrease in ionic current, causing an impedance peak to appear. In principle, the impedance peak amplitude should be linear to the volume of the particle (Choi et al., 2013; Chun et al., 2005; Guo et al., 2015b; Kim et al., 2009; Rho et al., 2018). At the same time, blue light irradiates the fluorescence detection region shown in Fig. 3(a) and excites the fluorescent molecules. The impedance and fluorescence signals were simultaneously obtained in the area shown in Fig. 3(a). The current chip design consists of dual outlets, enabling throughput to double that of a single outlet. Throughput can be defined as the amount of liquid that flows through the chip per second. Throughput is determined by the chip geometry, specifically the narrowest part of the chip, which is the sensing channel. Our chip design uses a dual channel to decrease the

total flow resistance by half, allowing the throughput to double. This allows analysis to be performed in half the time it takes with a single channel. The current design also simplifies chip fabrication by removing the need for gel, which was necessary in the previous designs.

3.3. DC impedance-based analysis of aerosolized microbeads and bacteria

The correlation between the impedance peak amplitude and microbead volume was assessed with aerosolized fluorescent microbeads of different diameters (0.96, 2.07, and 2.95 μm). The actual impedance data is presented in Fig. S2. The peak amplitudes and particle volumes obtained using the newly designed cytometer are plotted in Fig. 4(a). The calibration curve with a linearity of $R^2 = 0.9967$ proves that the principle fits well with this cytometer. A calibration curve was used to draw the histogram in Fig. 4(b). The diameters of the microbeads calculated from the peak intensities were clearly distinguishable from each other. *E. coli* BL21 was also measured, and the calculated diameters were plotted along with the beads in Fig. 4(b). The diameters and statistical calculations of the beads and *E. coli* are presented in Table S1. *E. coli* has a cylindrical structure with a hemispherical cap with a diameter of approximately 1 μm and a length of approximately 2 μm. The mean diameter of 1.641 μm calculated in Table S1 seems to be in good agreement with the actual value. A rather large standard deviation compared to those of beads comes from the actual inconsistencies in *E. coli* cell sizes (Yao et al., 2012). The cytometer was also used to deduce bead concentration successfully as presented in Fig. S3.

3.4. Quantification of aerosolized microbeads and bacteria

The efficiency of the bioaerosol detection system was evaluated with aerosolized 2.07 μm beads, as shown in Fig. 5(a). Beads were aerosolized for 1, 3, 5, 7, and 10 min to make different concentrations in the chamber, and the concentrations were measured with the spectrometer. Then, the air sampler collected the aerosolized beads into 10 mL DPBS solution for 5 min. Part of the solution was put through a DC impedance microfluidic cytometer and another part was measured with a BD FACS Canto™ II as a reference. Fig. 5(a) compares the total bead counts calculated from the three different measurements. Comparison of particle counts from the spectrometer and FACS elicited collection efficiency. The collection efficiency varied depending on the concentration and was 28.04% on average. This is because of two factors, the inaccuracy of aerosol spectrometer and sedimentation/adsorption of aerosol during collection. First, aerosol spectrometer measures all particles including water droplets. Therefore, overestimation is expected. Secondly, sedimentation occurs as can be seen in Fig. 2(b). However, direct comparison of spectrometer and cyclone-cytometer integrated air monitor (CCAM) is inappropriate because they have different purpose. Unlike spectrometer which measures concentration of all airborne matter, CCAM aims to capture and measure specific low concentration pathogen in the air. Comparison of particle counts from FACS and DC impedance cytometry elicited detection efficiency. The detection efficiency was 87.68% on an average. The 12.32% loss could be due to the dead volume in the inlet reservoir. The syringe pump cannot push the entire solution through the detector. Part of the solution remains after the pump is completely pushed forward. This could be improved by making the reservoir smaller or the entire channel length shorter to reduce the dead volume. The overall device efficiency was calculated by comparing the spectrometer measurements and DC impedance cytometer measurements, which was 24.59% on average. The device could be said to perform efficiently over the tested particle concentration range.

The device efficiency was also observed in *E. coli*. *E. coli* was diluted in DPBS solution when aerosolized to preserve the structure of *E. coli*. Because of the dried salts produced from the DPBS solution, the concentration of particles in the air could not be measured accurately, so the spectrometer data is missing from the *E. coli* measurement. Fig. 5(b) compares the results from FACS and the microfluidic cytometer. The concentrations of *E. coli* solution measured by the microfluidic cytometer were, on average, 81.61% compared to the concentration measured by FACS. The reason for the low concentration of bacteria compared to microbeads might be (1) *E. coli* tends to adhere to the wall of the microfluidic channel and (2) the diameter of *E. coli* was smaller than that of beads and might be less efficient at the collection step. For these reasons, the data measured here supports the usefulness of combining the cyclone sampler with a microfluidic cytometer for reasonably fast detection of the target microbial cells in bioaerosols.

3.5. Differentiation of dust, live E. coli, and dead E. coli

Finally, CCAM device was utilized of its specific pathogen detecting ability. The device was used to differentiate dust, live bacteria, and dead bacteria by the addition of bacteria staining dye in a wet cyclone sampling liquid. LIVE/DEAD® BacLight™ was used to stain live bacteria green and dead bacteria red. LIVE/DEAD® BacLight™ is a mixture of two nucleic acid stains, SYTO 9 and propidium iodide. SYTO 9 green fluorescent dye stains all bacterial populations. In contrast, propidium iodide red-fluorescent dye stains only bacteria with damaged membranes, causing a reduction in SYTO 9 green fluorescence. *E. coli* was used as the model bacteria in this experiment. Microscopic image of dust, live *E. coli*, and dead *E. coli* mixed with BacLight reagent is shown in Fig. S4. The actual device operation was executed with individual

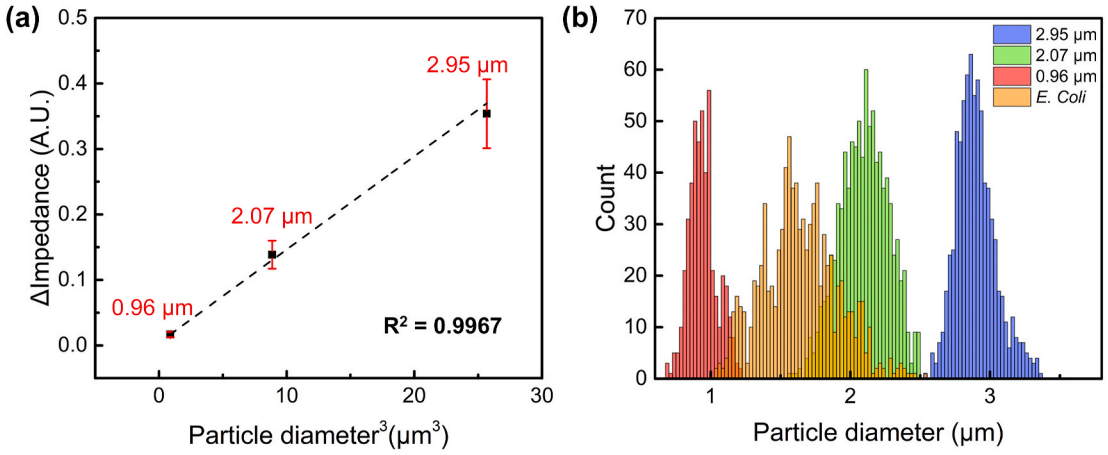

Fig. 4. (a) Peak amplitudes of the DC impedance signal from microbeads (0.96, 2.07, and 2.95 μm in diameter) plotted against particle volume. Peak amplitude and the cube of particle diameter calibration curve shows near-linear relation with R^2 of 0.9967. (b) Histogram of the diameter calculated with the calibration curve for *E. coli* and the three types of microbeads.

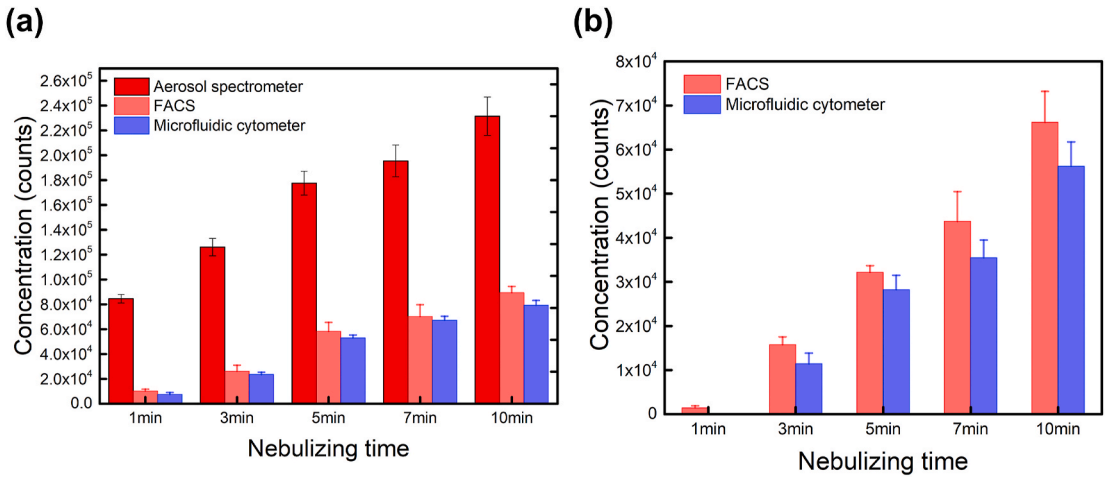

Fig. 5. (a) Results of concentration measurement of collected microbeads (2.07 μm in diameter) using air sampler in the air chamber. Quantification is carried out with commercial aerosol spectrometer, microfluidic cytometer, and commercial FACS. (b) Results of concentration measurement of collected *E. coli* using air sampler in the air chamber. Quantification is carried out with microfluidic cytometer and commercial FACS.

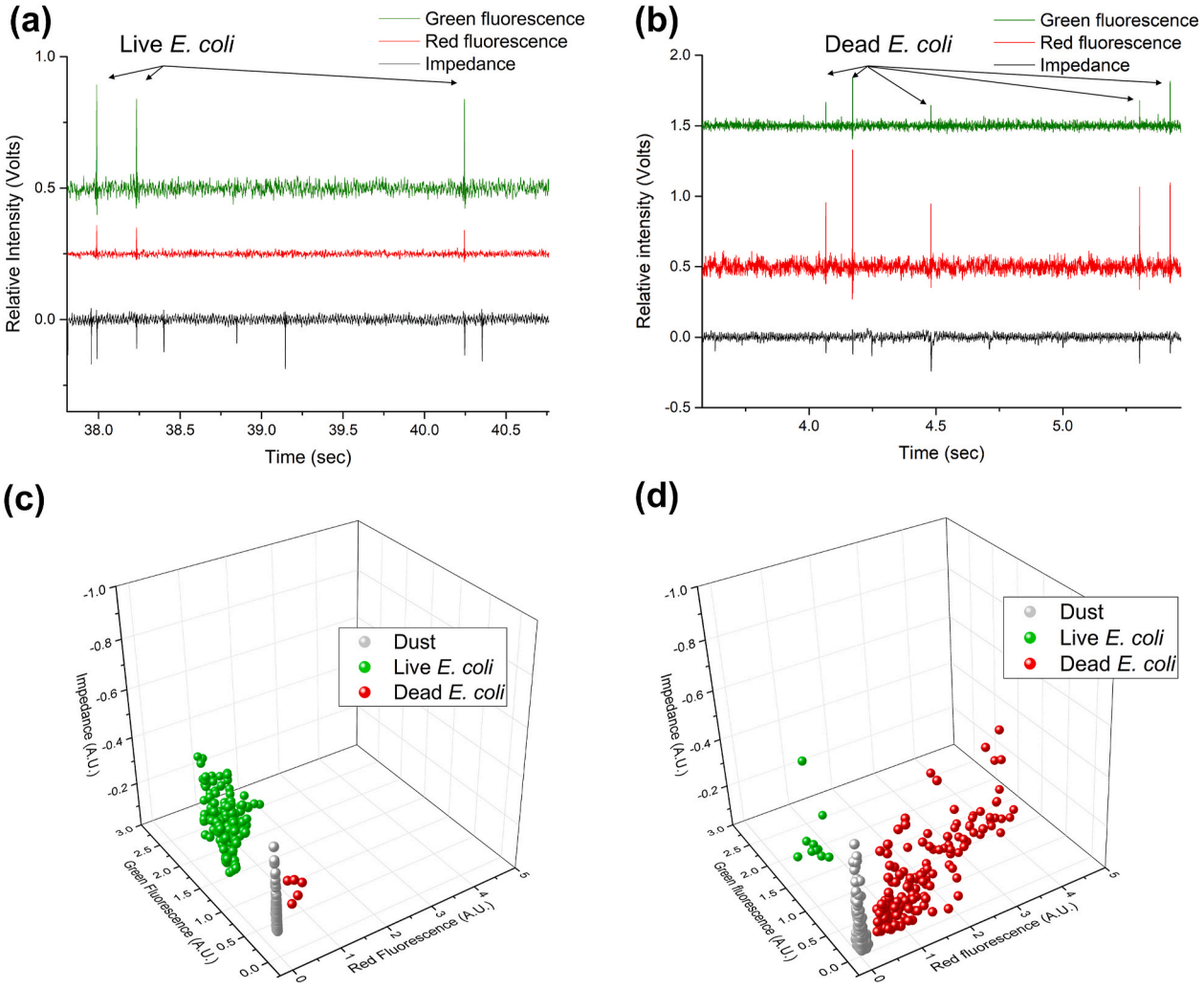

Fig. 6. Detection of dust, live *E. coli*, and dead *E. coli* when sampled in BacLight reagent containing solution. (a) DC impedance cytometer impedance and fluorescence data of dust and live *E. coli* (b) DC impedance cytometer impedance and fluorescence data of dust and dead *E. coli* (c) 3-dimensional plot of cytometer data for live *E. coli* (d) 3-dimensional plot of cytometer data for dead *E. coli*.

samples containing dust mixed with either live *E. coli* or dead *E. coli*. Fig. 6(a) shows the simultaneous impedance and fluorescence signals of live *E. coli* with clear green fluorescence. The ratio of green to red fluorescence was high enough to identify them as live. Fig. 6(b) shows the impedance and fluorescence measurements of dead *E. coli* mixed with dust, and the relatively high red fluorescence clearly shows that *E. coli* is dead. Fig. 6(c) and (d) show 3-dimensional plots of impedance, green fluorescence, and red fluorescence from live and dead *E. coli* samples. The differences in the populations of green and red fluorescence clearly distinguishes whether the majority of cells are dead or alive. The simple addition of reagents to the sampling liquid has allowed the determination of whether bacteria have lost their virulence. This could be used to measure the effective concentration of pathogens that can infect people. Further identification can take place by simply exchanging fluorescent label or other methods depending on the target of interest and the purpose (Iswardy et al., 2017; Lippe, 2018).

4. Conclusions

We constituted the first air monitoring system to utilize DC impedance for particle size measurement. The air monitoring system consisted of a wet cyclone air sampler for aerosol collection and a DC impedance microfluidic cytometer for bacteria detection. CCAM was designed to not require any separate pretreatment for bacteria detection. CCAM was verified using microbeads, dust, and *Escherichia coli*. The device was able to measure the concentration of the collected particles to $\sim 1 \times 10^3$ particle mL^{-1}. CCAM was able to collect particles in the air with an average collection efficiency of 28.04%. The high collection efficiency and detection efficiency in this study demonstrate the potential of the proposed device as a real-time air monitoring system. Based on the confirmed efficiency, the device successfully differentiated dust and live/dead *E. coli* using the well-known BacLight LIVE/DEAD reagent. This is not a mere specific analyzer but an analytical platform that could be utilized for a variety of purposes. To determine the bacterial cell wall type, a gram stain reagent was used in this work. However, the usage could be further extended to a more specific determination of species with the introduction of antibody-fluorescence molecules. The proposed platform is the basis for the air-monitoring system for out-of-the-lab use that will be useful in the near future.

CRediT authorship contribution statement

Chang Heon Lee: Formal analysis, Investigation, Writing – original draft, Writing – review & editing. **Hyunho Seok:** Formal analysis, Writing – original draft, Writing – review & editing. **Woohyuk Jang:** Conceptualization, Formal analysis, Investigation, Writing – original draft, Visualization. **Ji Tae Kim:** Investigation, Writing – review & editing. **Geunsang Park:** Writing – review & editing. **Hyeong-U Kim:** Writing – review & editing. **Jihun Rho:** Writing – review & editing. **Taesung Kim:** Writing – review & editing, Supervision, Funding acquisition. **Taek Dong Chung:** Writing – review & editing, Supervision, Project administration, Funding acquisition.

Declaration of competing interest

The authors declare that they have no known competing financial interests or personal relationships that could have appeared to influence the work reported in this paper.

Acknowledgements

This work was supported by the National Research Foundation of Korea (NRF) grant funded by the Korean government (MSIT) [2017R1E1A1A01074236]; the National Research Foundation of Korea (NRF) funded by the Ministry of Education [2018R1D1A1B07040292] [2016M3A7B4909649]; the Ministry of Trade, Industry & Energy [20011101]; the Korea Medical Device Development Fund grant funded by the Korea government [NTIS Number: 1711138201]. This research was partially supported by NST/KIMM, Republic of Korea.

Appendix A. Supplementary data

Supplementary data to this article can be found online at https://doi.org/10.1016/j.bios.2021.113499.

References

Ateya, D.A., Erickson, J.S., Howell, P.B., Hilliard, L.R., Golden, J.P., Ligler, F.S., 2008. The good, the bad, and the tiny: a review of microflow cytometry. Anal. Bioanal. Chem. 391, 1485–1498. https://doi.org/10.1007/s00216-007-1827-5.

Caruana, D.J., 2011. Detection and analysis of airborne particles of biological origin: present and future. Analyst 136, 4641. https://doi.org/10.1039/c1an15506g.

Chen, P.S., Li, C.S., 2005. Sampling performance for bioaerosols by flow cytometry with fluorochrome. Aerosol Sci. Technol. 39, 231–237. https://doi.org/10.1080/027868290925534.

Choi, H., Jeon, C.S., Hwang, I., Ko, J., Lee, S., Choo, J., Boo, J.-H., Kim, H.C., Chung, T. D., 2014. A flow cytometry-based submicron-sized bacterial detection system using a movable virtual wall. Lab Chip 14, 2327–2333. https://doi.org/10.1039/c4lc00238e.

Choi, H., Kim, K.B., Jeon, C.S., Hwang, I., Lee, S., Kim, H.K., Kim, H.C., Chung, T.D., 2013. A label-free DC impedance-based microcytometer for circulating rare cancer cell counting. Lab Chip 13, 970–977. https://doi.org/10.1039/c2lc41376k.

Choi, J., Kang, M., Jung, J.H., 2015. Integrated micro-optofluidic platform for real-time detection of airborne microorganisms. Sci. Rep. 5, 15983. https://doi.org/10.1038/srep15983.

Chun, H., Chung, T.D., Kim, H.C., 2005. Cytometry and velocimetry on a microfluidic chip using polyelectrolytic salt bridges. Anal. Chem. 77, 2490–2495. https://doi.org/10.1021/ac048535o.

Fu, Y., Yuan, Q., Guo, J., 2017. Lab-on-PCB-based micro-cytometer for circulating tumor cells detection and enumeration. Microfluid. Nanofluidics 21, 20. https://doi.org/10.1007/s10404-017-1854-2.

Ghosh, B., Lal, H., Srivastava, A., 2015. Review of bioaerosols in indoor environment with special reference to sampling, analysis and control mechanisms. Environ. Int. 85, 254–272. https://doi.org/10.1016/j.envint.2015.09.018.

Guo, J., Ai, Y., Cheng, Y., Li, C.M., Kang, Y., Wang, Z., 2015a. Volumetric measurement of human red blood cells by MOSFET-based microfluidic gate. Electrophoresis 36, 1862–1865. https://doi.org/10.1002/elps.201400365.

Guo, J., Chen, L., Ai, Y., Cheng, Y., Li, C.M., Kang, Y., Wang, Z., 2015b. Numerical and experimental characterization of solid-state micropore-based cytometer for detection and enumeration of biological cells. Electrophoresis 36, 737–743. https://doi.org/10.1002/elps.201400376.

Huffman, J.A., Perring, A.E., Savage, N.J., Clot, B., Crouzy, B., Tummon, F., Shoshanim, O., Damit, B., Schneider, J., Sivaprakasam, V., Zawadowicz, M.A., Crawford, I., Gallagher, M., Topping, D., Doughty, D.C., Hill, S.C., Pan, Y., 2020. Real-time sensing of bioaerosols: review and current perspectives. Aerosol Sci. Technol. 54, 465–495. https://doi.org/10.1080/02786826.2019.1664724.

Hurley, J., 1970. Sizing particles with a coulter counter. Biophys. J. 10, 74–79. https://doi.org/10.1016/S0006-3495(70)86286-5.

Iswardy, E., Tsai, T.-C., Cheng, I.-F., Ho, T.-C., Perng, G.C., Chang, H.-C., 2017. A bead-based immunofluorescence-assay on a microfluidic dielectrophoresis platform for rapid dengue virus detection. Biosens. Bioelectron. 95, 174–180. https://doi.org/10.1016/j.bios.2017.04.011.

Joo, S., Kim, K.H., Kim, H.C., Chung, T.D., 2010. A portable microfluidic flow cytometer based on simultaneous detection of impedance and fluorescence. Biosens. Bioelectron. 25, 1509–1515. https://doi.org/10.1016/j.bios.2009.11.011.

Kalogerakis, N., Paschali, D., Lekaditis, V., Pantidou, A., Eleftheriadis, K., Lazaridis, M., 2005. Indoor air quality—bioaerosol measurements in domestic and office premises. J. Aerosol Sci. 36, 751–761. https://doi.org/10.1016/j.jaerosci.2005.02.004.

Kim, H.-U.U., Min, J., Park, G., Shin, D., Sung, G., Kim, T., Lee, M.-H.H., 2018. Electrochemical detection of airborne influenza virus using air sampling system. Aerosol Air Qual. Res. 18, 1–7. https://doi.org/10.4209/aaqr.2018.06.0221.

Kim, K.B., Chun, H., Kim, H.C., Chung, T.D., 2009. Red blood cell quantification microfluidic chip using polyelectrolytic gel electrodes. Electrophoresis 30, 1464–1469. https://doi.org/10.1002/elps.200800448.

Kman, N.E., Bachmann, D.J., 2012. Biosurveillance: a review and update. Adv. Prev. Med. 1–9. https://doi.org/10.1155/2012/301408, 2012.

Lange, J.L., Thorne, P.S., Lynch, N., 1997. Application of flow cytometry and fluorescent in situ hybridization for assessment of exposures to airborne bacteria. Appl. Environ. Microbiol. 63, 1557–1563.

Levin, P.A., Angert, E.R., 2015. Small but mighty: cell size and bacteria. Cold Spring Harb. Perspect. Biol. 7, 1–11. https://doi.org/10.1101/cshperspect.a019216.

Lippe, R., 2018. Flow virometry: a powerful tool to functionally characterize viruses. J. Virol. 92 https://doi.org/10.1128/JVI.01765-17.

Liu, Y., Daum, P.H., 2000. The effect OF refractive index ON size distributions and light scattering coefficients derived from optical particle counters. J. Aerosol Sci. 31, 945–957. https://doi.org/10.1016/S0021-8502(99)00573-X.

McClain, M.A., Culbertson, C.T., Jacobson, S.C., Ramsey, J.M., 2001. Flow cytometry of Escherichia coli on microfluidic devices. Anal. Chem. 73, 5334–5338. https://doi.org/10.1021/ac010504v.

Miller, B.V., Limes, R.W., 1988. Recent advances in particle size measurements: a critical review. CRC Crit. Rev. Anal. Chem. 20, 75–116. https://doi.org/10.1080/00078988808048808.

Minogue, T.D., Koehler, J.W., Stefan, C.P., Conrad, T.A., 2019. Next-generation sequencing for biodefense: biothreat detection, forensics, and the clinic. Clin. Chem. 65, 383–392. https://doi.org/10.1373/clinchem.2016.266536.

Morales-Narváez, E., Dincer, C., 2020. The impact of biosensing in a pandemic outbreak: COVID-19. Biosens. Bioelectron. 163, 112274. https://doi.org/10.1016/j.bios.2020.112274.

Nazaroff, W.W., 2016. Indoor bioaerosol dynamics. Indoor Air 26, 61–78. https://doi.org/10.1111/ina.12174.

Prigione, V., Lingua, G., Filipello Marchisio, V., 2004. Development and use of flow cytometry for detection of airborne fungi. Appl. Environ. Microbiol. 70, 1360–1365. https://doi.org/10.1128/AEM.70.3.1360-1365.2004.

Qin, Z., Zhe, J., Wang, G.-X., 2011. Effects of particle's off-axis position, shape, orientation and entry position on resistance changes of micro Coulter counting devices. Meas. Sci. Technol. 22, 045804 https://doi.org/10.1088/0957-0233/22/4/045804.

Ren, C., Zhang, S., Song, D., Jinhong, G., 2016. Lab on dielectric film deposited PCB device for characterization of electrical property of biological cells. IEEE Trans. Dielectr. Electr. Insul. 23, 1895–1897. https://doi.org/10.1109/TDEI.2016.7556459.

Rho, J., Jang, W., Hwang, I., Lee, D., Lee, C.H., Chung, T.D., 2018. Multiplex immunoassays using virus-tethered gold microspheres by DC impedance-based flow cytometry. Biosens. Bioelectron. 102, 121–128. https://doi.org/10.1016/j.bios.2017.11.027.

Rosenberg, P.D., Dean, A.R., Williams, P.I., Dorsey, J.R., Minikin, A., Pickering, M.A., Petzold, A., 2012. Particle sizing calibration with refractive index correction for light scattering optical particle counters and impacts upon PCASP and CDP data collected during the Fennec campaign. Atmos. Meas. Tech. 5, 1147–1163. https://doi.org/10.5194/amt-5-1147-2012.

Shrirao, A.B., Fritz, Z., Novik, E.M., Yarmush, G.M., Schloss, R.S., Zahn, J.D., Yarmush, M.L., 2018. Microfluidic flow cytometry: the role of microfabrication methodologies, performance and functional specification. Technology 6, 1–23. https://doi.org/10.1142/s2339547818300019.

Stier, J., Quinten, M., 1998. Simple refractive index correction for the optical particle counter PCS 2000 by Palas. J. Aerosol Sci. 29, 223–225. https://doi.org/10.1016/S0021-8502(97)00459-X.

Sung, G., Ahn, C., Kulkarni, A., Shin, W.G., Kim, T., 2017. Highly efficient in-line wet cyclone air sampler for airborne virus detection. J. Mech. Sci. Technol. 31, 4363–4369. https://doi.org/10.1007/s12206-017-0835-4.

Whitesides, G.M., 2006. The origins and the future of microfluidics. Nature 442, 368–373. https://doi.org/10.1038/nature05058.

Xu, Z., Wu, Y., Shen, F., Chen, Q., Tan, M., Yao, M., 2011. Bioaerosol science, technology, and engineering: past, present, and future. Aerosol Sci. Technol. 45, 1337–1349. https://doi.org/10.1080/02786826.2011.593591.

Yao, Z., Davis, R.M., Kishony, R., Kahne, D., Ruiz, N., 2012. Regulation of cell size in response to nutrient availability by fatty acid biosynthesis in Escherichia coli. Proc. Natl. Acad. Sci. Unit. States Am. 109, E2561–E2568. https://doi.org/10.1073/pnas.1209742109.